COMMUNICATION

Electronic Supplementary Information

Manipulating light trapping and water vaporization enthalpy via porous hybrid nanohydrogel for enhanced solar-driven interfacial water evaporation with antibacterial ability

Yaling Li,[a] Mingyu Zhao,[a] Yunshi Xu,[a] Leilei Chen,[b] Ting Jiang,[b] Weicun Jiang,[a] Shuguang Yang*,[a] and Yi Wang*,[a,b]

[a] Center for Advanced Low-dimension Materials & State Key Laboratory for Modification of Chemical Fibers and Polymer Materials, College of Material Science and Engineering, Donghua University, Shanghai 201620, China. E-mail: shgyang@dhu.edu.cn, ywang@dhu.edu.cn

[b] College of Chemistry, Chemical Engineering and Biotechnology, Donghua University, Shanghai 201620, China

Experimental Section

Materials. Ammonium tetrathiomolybdate ($(NH_4)_2MoS_4$) was purchased from Sigma-Aldrich (Shanghai) Trading Co., Ltd (Shanghai, China). Hydrazine monohydrate ($N_2H_4{\cdot}H_2O$, 98%) was purchased from TCI (Shanghai) Development Co., Ltd. Polyethylene imine (PEI, molecular weight = 70,000, 50% aqueous solution) and less layer molybdenum (diameter: 0.2-10 μm, number of layers: 1-10) were purchased from Aladdin Chemistry Co., Ltd. (China). Mixed cellulose esters (MCE) membrane (pore size around 0.22 μm) was purchased from Lubitech Technologies Ltd. (Shanghai, China) and cut into small round pieces (diameter: 2.3 cm). All chemicals were used without further purification. Deionized water was obtained from a laboratory water purification system and used in all experiments.

Characterization. Scanning electron microscopy (SEM) measurements were performed on a Hitachi SU 8010 field emission SEM. Transmission electron microscopy (TEM) and high resolution TEM (HRTEM) images were recorded with a JEOL 2100 F equipment. X-ray photoelectron spectra (XPS) were obtained by an Escalab 250Xi system. UV-Vis spectra were collected on a Shimadzu UV-2550 spectrophotometer. UV-Vis-NIR absorption and reflectance spectra of samples were recorded on a spectrometer (Lambda 950) equipped with an integration sphere. Nitrogen adsorption/desorption isotherms were tested on ASAP 2020 and the specific surface area and pore diameter distribution were calculated by Brunauer-Emmett-Teller method (BET) and Barrett-Joyner-Halenda method (BJH), respectively. Raman spectra were performed using a laser Raman spectrometer excited with a 532 nm laser. Water contact

angle measurements were carried on an OCA 40 Micro optical contact angle measuring system using a droplet of 3 μL water as indicator. The thermal images of the absorbers were captured by FOTRIC 225 infrared camera. Zeta potentials were measured on a Malvern Zetasizer Nano ZS system. Thermogravimetric analysis (TGA) was obtained on a Discovery TGA 550 system with the nitrogen atmosphere. The mechanical tests were collected on an electronic universal testing machine (Shengzhen SUNS Technology stock Co. LTD.) with a tensile rate of 50 mm min^{-1}. Solar evaporation tests were carried out with a xenon lamp (CEL-HXF300, Education Au-light Co., Beijing, China).

Synthesis of MoS_2 nanoflowers. MoS_2 nanoflowers were synthesized by a one-step, hydrothermal reaction. Briefly, 55 mg of $(NH_4)_2MoS_4$ powder was dispersed in 25 mL of H_2O via stirring and ultrasonic for 30 min, which was followed by the addition of 0.25 mL of $N_2H_4{\cdot}H_2O$ and further ultrasonic for 30 min. Then the mixture was transferred into a 100 mL Teflon-lined autoclave to react at 200 °C for over 10 h. The black product was collected by centrifugation at 10000 rpm for 5 min and subsequently washed with DI water. The washing step was repeated for at least 10 times to remove unreacted reagents. Finally, the final product was lyophilized for future use.

Fabrication of MoS_2@PEI/MCE. MoS_2@PEI/MCE composite membrane was prepared via a home-made vacuum filtration method. Briefly, 2 mg MoS_2 was dispersed into deionized water with 1 mg PEI. Then, the dispersion was filtrated onto MCE membrane via vacuum filtration to obtain MoS_2@PEI/MCE bi-layered membrane. PEI/MCE and MoS_2/MCE could be accordingly prepared without the addition of MoS_2 or PEI. To optimize the membrane formation, comparative trial MoS_2@PEI/MCE membranes were prepared with different amounts of PEI (0, 0.2, 0.5, 1, 2, 4 mg) or MoS_2 (0, 1.5, 3.0, 4.5, 6.0 mg) through the same procedure. Correspondingly, MoS_2@PEI/MCE membranes with variable thickness of top MoS_2 layer could be facilely prepared using different concentrations of MoS_2@PEI aqueous solution with a fixed mass ratio of PEI and MoS_2 (PEI : MoS_2 = 1 : 2). Herein, M1 (0.25 mg/mL MoS_2 and 0.125 mg/mL PEI), M2 (0.5 mg/mL MoS_2 and 0.25 mg/mL PEI), M3 (1 mg/mL MoS_2 and 0.5 mg/mL PEI), M4 (2 mg/mL MoS_2 and 1 mg/mL PEI), M5 (4 mg/mL MoS_2 and 2 mg/mL PEI) were used in the fabrication.

Saturated water adsorption, water evaporation rate, water state and vaporization enthalpy measurements. The pristine MoS_2 and MoS_2@PEI nanoparticles were collected by centrifugation at 10000 rpm for 5 min and subsequently washed with DI water. The final products were lyophilized as MoS_2-dry and MoS_2@PEI-dry for TGA tests. Meanwhile, the residual final products were kept in a dry tower under the saturated vapor pressure for 60 h at 35 °C and then acted as MoS_2-wet and MoS_2@PEI-wet for saturated water adsorption measurements during the TGA tests. The water evaporation rate measurements were performed with MoS_2-wet and MoS_2@PEI-wet under the constant temperature at 50 °C with TGA measurements. The water state of water confined in PEI-mediated nanohydrogel network was performed by the Raman spectrometer excited with a 532 nm laser. The Raman spectra were fitted by Gaussian function. The differential scanning calorimetry (DSC) measurements with 5 °C/min heating rate, under nitrogen flow flux (50 mL min^{-1}), in the temperature range from 30 to 180 °C were investigated for calculating the vaporization energy of blank water and water in the nanohydrogel. The measured enthalpy of water is 2369 J/g, which is close to the theoretical value of 2444 J/g,[11] indicating the accuracy of our measurements.

Solar pervaporation performance measurement. The xenon lamp with a light power density of 3.7 kW m^{-2} was used to simulate solar irradiation. The beaker contained 24 mL water and varieties of membranes floated on it for the measurements. The solar pervaporation activity of membranes was evaluated by monitoring the mass change of water in the beaker by an electronic balance with an accuracy of 0.01 g during a certain time irradiation. To confirm the reusability and stability of the membrane, the same membrane was used for at least ten cycles (environment average humidity is 63%).

The formula $\eta = vH_e/Q_s$ can be used for calculating the photothermal evaporation efficiency (η), where v is the water evaporation rate (obtained from the slope of the steady-state mass change curves), H_e is the total enthalpy of sensible heat and phase change of liquid to water and Q_s is the power density of solar illumination.[1,2] The average evaporation rate of pure water in the dark environment is subtracted when calculating the photothermal water evaporation efficiency.[3,4]

***Antibacterial test*.** Gram-negative bacteria, Escherichia coli (E. coli), were selected as bacterial models. Firstly, the raw materials (PEI and MoS_2) were tested with antibacterial performances. Typically, PEI, MoS_2 and MoS_2@PEI aqueous solutions before filtration onto the MCE were added into a sterile centrifugal tube containing certain bacterial suspension, respectively. The tubes were then shaken at 37 °C for 16 h. After that, the bacterial suspensions were taken out and diluted for the optical density (OD) test. At the same time, the PEI, MoS_2 and MoS_2@PEI aqueous solutions were dripped onto the agar plate containing 100 μL diluted bacterial suspension, respectively. The plates were incubated for 18 h at 37 °C to show bacterial colonies growth. Secondly, diverse membrane samples (MCE, PEI/MCE, MoS_2/MCE and MoS_2@PEI/MCE) were placed onto the agar plate containing 100 μL diluted bacterial suspension and incubated for 24 h at 37 °C. To directly observe the bacteriostatic effect, the membrane samples were fixed and prepared for SEM measurements. Furthermore, the various membrane samples were placed in conical flasks and then the E. coli suspension was pipetted onto the surface of the membranes. After 12 h contact period at 37 °C, the suspensions were diluted with sterile distilled water and they were plated with agar and incubated for 24 h at 37 °C to corroborate the bacteriostatic efficacy. Finally, the E. coli bacterial suspension with a certain amount of MoS_2 was illuminated for seven minutes and the blank bacterial suspension was used for comparison. The corresponding bacterial suspensions before and after illumination were plated with agar and incubated for 24 h at 37 °C to verify the photothermal synergistic antibacterial effect of MoS_2.

Supplementary Figure

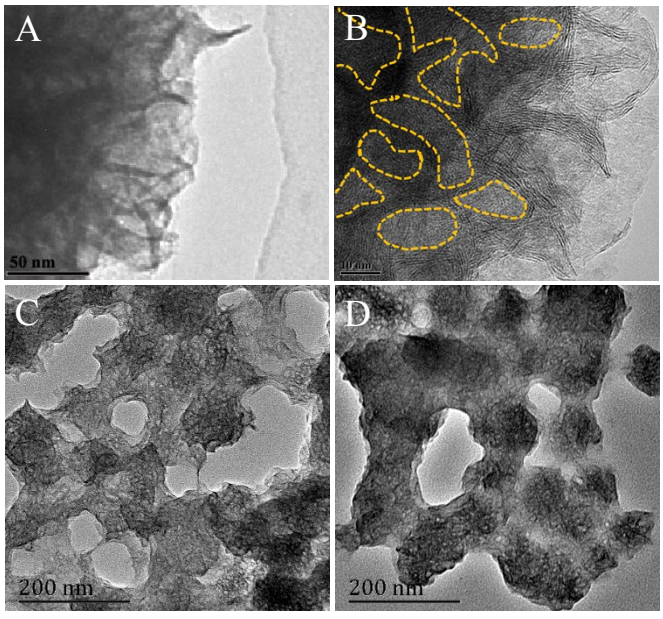

Fig. S1 TEM images of (A, B) MoS_2 nanoflowers and (C, D) MoS_2@PEI nanohydrogels.

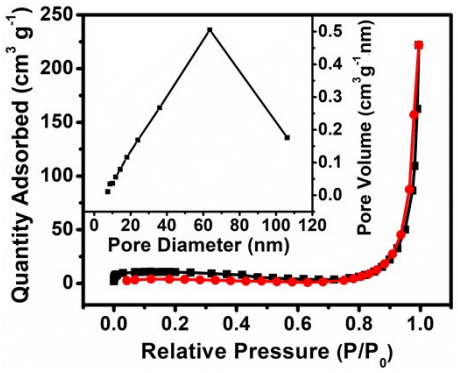

Fig. S2 Nitrogen adsorption-desorption isotherms and pore size distribution curve (inset) of MoS_2 nanoflowers.

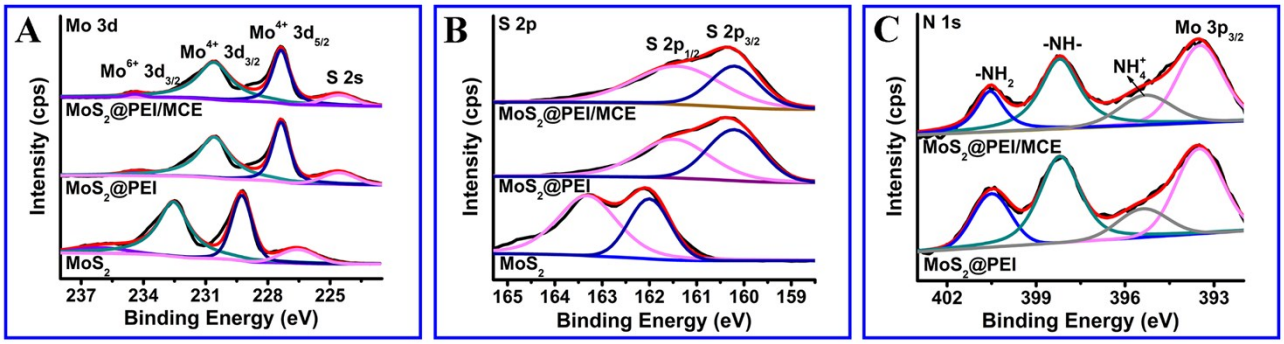

Fig. S3 (A-C) High-resolution XPS scans of (D) Mo 3d, (E) S 2p and (F) N 1s.

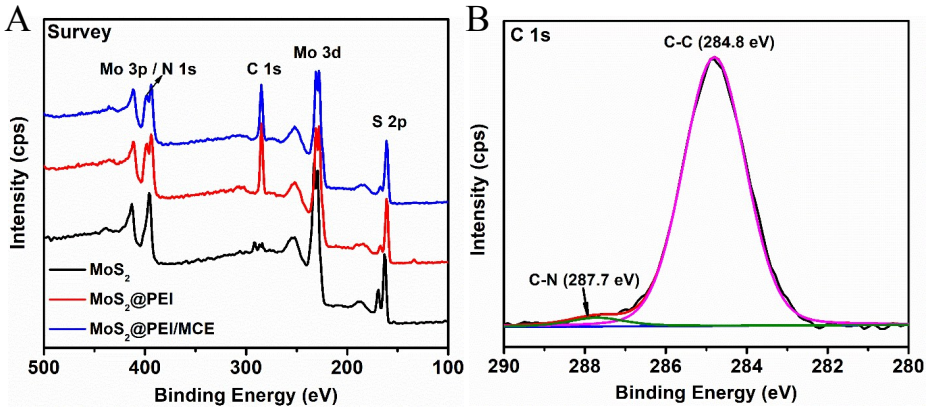

Fig. S4 (A) XPS spectra of MoS_2, MoS_2@PEI and MoS_2@PEI/MCE membrane and (B) high-resolution XPS scan of C 1s of MoS_2@PEI.

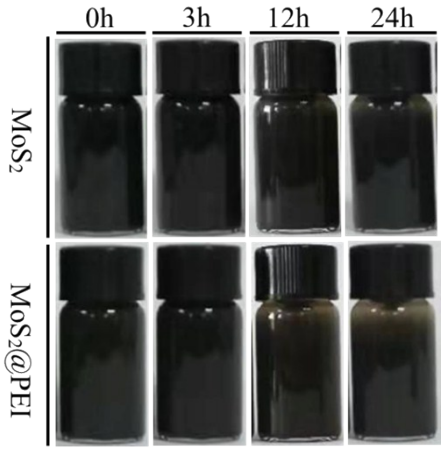

Fig. S5 Optical images of MoS_2 and MoS_2@PEI aqueous solution after standing for different time periods.

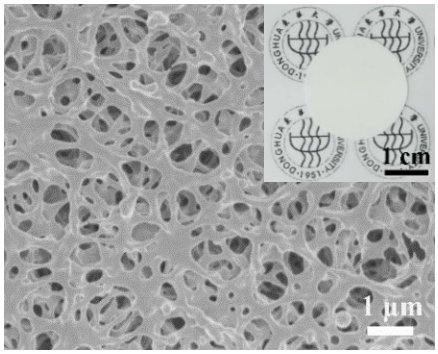

Fig. S6 Top-viewed SEM images and corresponding optical photo (inset) of MCE.

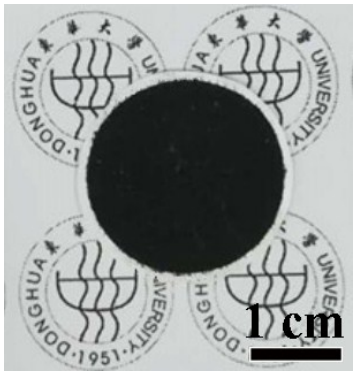

Fig. S7 Optical photo of MoS_2@PEI/MCE membrane.

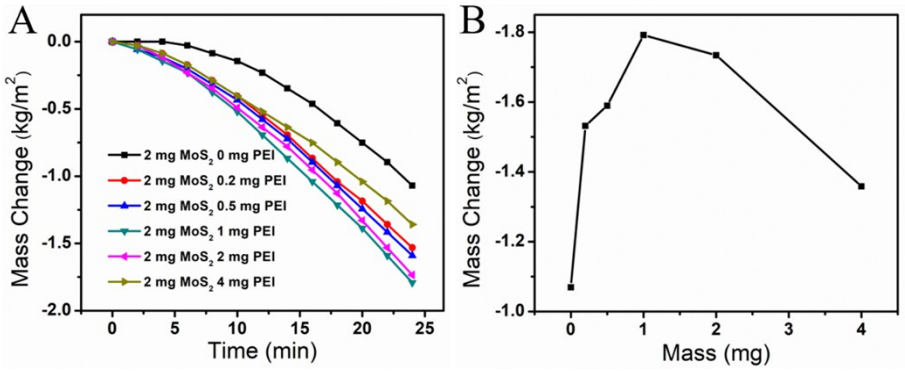

Fig. S8 (A, B) water evaporation performances under the simulated solar irradiation of MoS_2@PEI/MCE membranes with different amounts of PEI and a fixed amount of MoS_2.

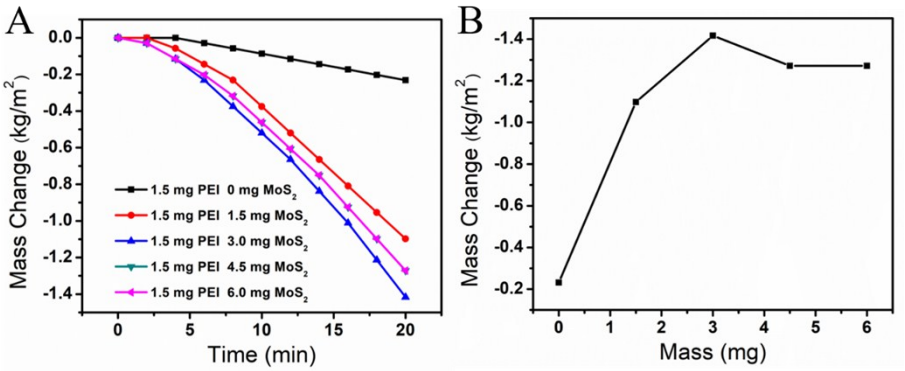

Fig. S9 (A, B) water evaporation performances under the simulated solar irradiation of MoS_2@PEI/MCE membranes with different amounts of MoS_2 and a fixed amount of PEI.

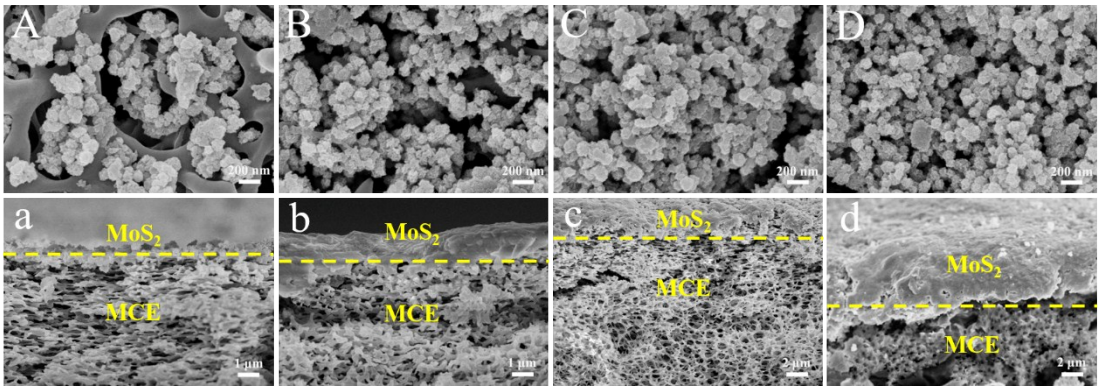

Fig. S10 (A-D) Top-viewed (Up) and (a-d) cross section-viewed (Bottom) SEM images of MoS_2@PEI/MCE membranes with different MoS_2 layer thickness of (A, a) M1, (B, b) M2, (C, c) M4 and (D, d) M5.

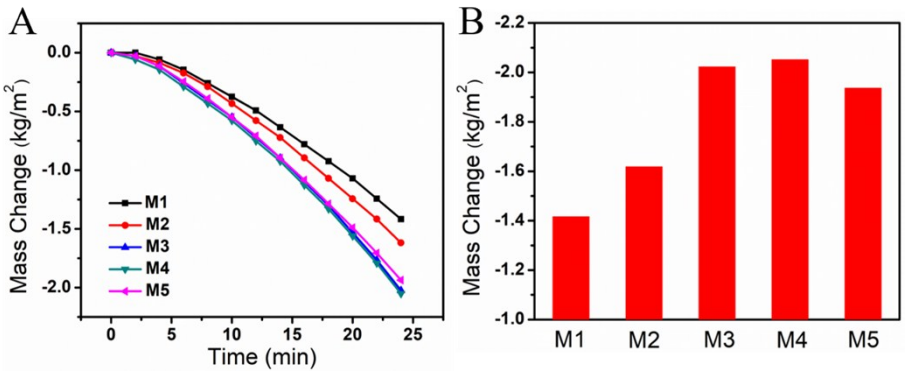

Fig. S11 (A, B) water evaporation performances under the simulated solar irradiation of MoS_2@PEI/MCE membranes with different MoS_2 layer thickness.

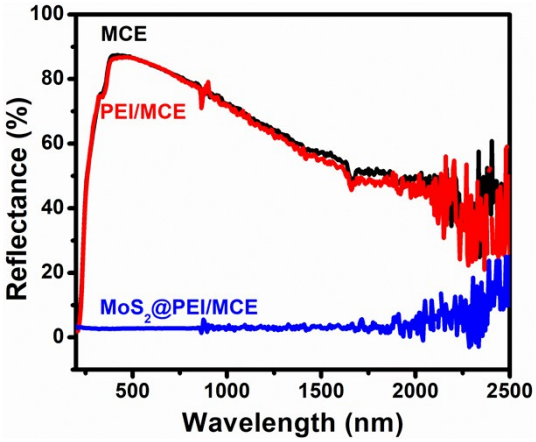

Fig. S12 UV-Vis-NIR reflectance spectra of MCE, PEI/MCE and MoS_2@PEI/MCE.

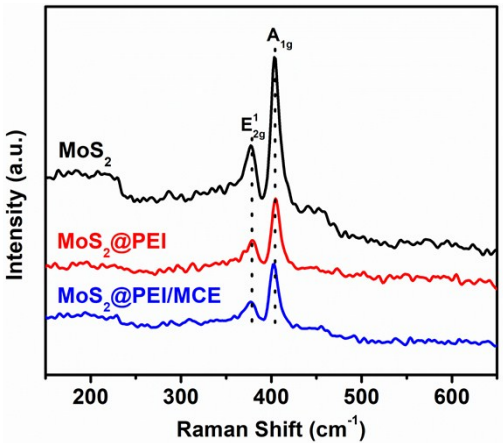

Fig. S13 Raman spectra of MoS_2, MoS_2@PEI and MoS_2@PEI/MCE.

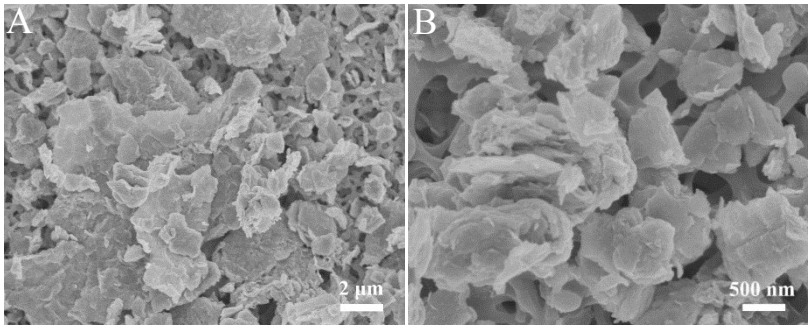

Fig. S14 SEM images of MoS_2@PEI/MCE prepared with MoS_2 nanosheets at different magnifications.

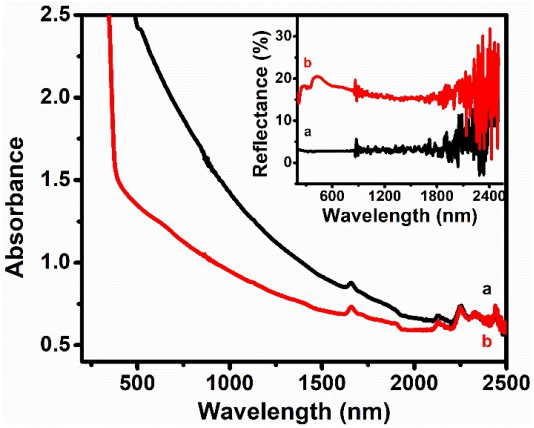

Fig. S15 UV-Vis-NIR absorption and reflectance spectra (inset) of (a) MoS_2(NF)@PEI/MCE and (b) MoS_2(NS)@PEI/MCE membranes.

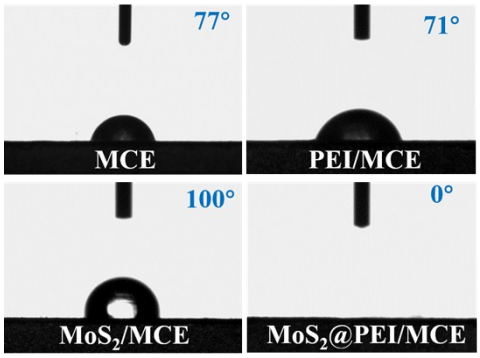

Fig. S16 Water contact angles of varied membranes.

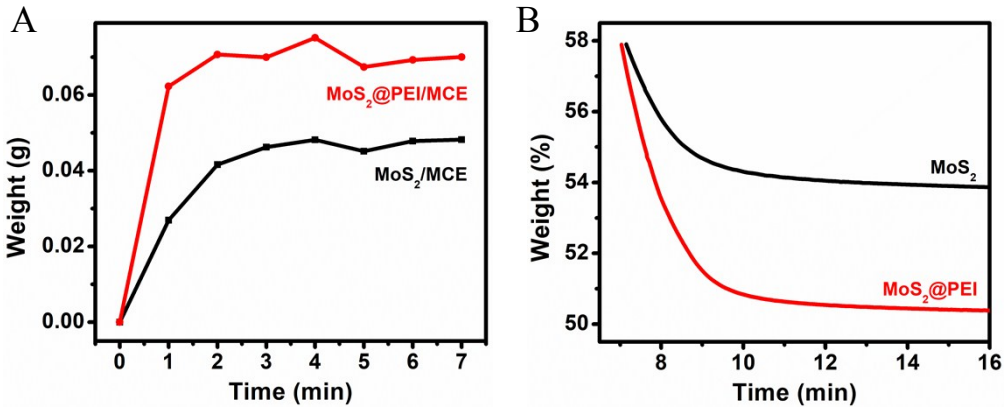

Fig. S17 (A) Water adsorption curves of MoS_2/MCE and MoS_2@PEI/MCE membranes over time under 50 °C. (B) Water evaporation curves of hydrous MoS_2 and MoS_2@PEI nanoparticles over time under 50 °C.

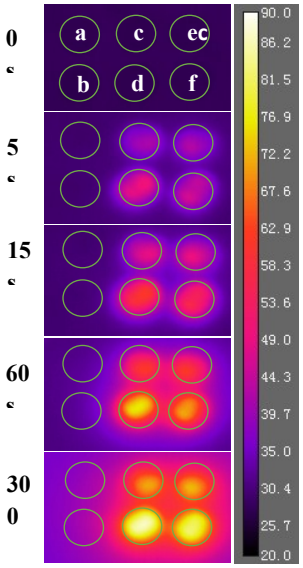

Fig. S18 IR thermal images of (a) MCE, (b) PEI/MCE, (c) MoS_2(NS)/MCE, (d) MoS_2(NF)/MCE, (e) MoS_2(NS)@PEI/MCE and (f) MoS_2(NF)@PEI/MCE membranes under a simulated solar irradiation (0.37 W/cm^{-2}) for different times.

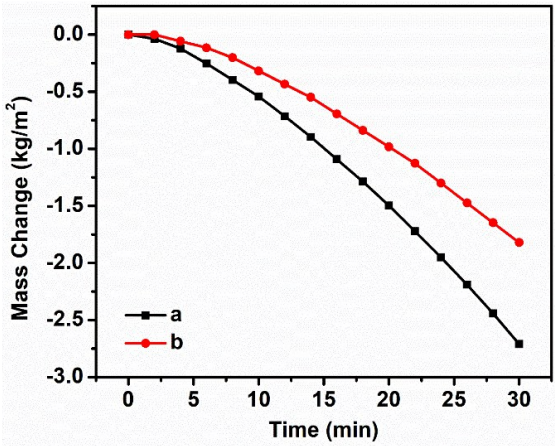

Fig. S19 Water evaporation performances under the simulated solar irradiation of MoS_2@PEI/MCE membranes prepared with (a) MoS_2 nanoflowers and (b) MoS_2 nanosheets, respectively.

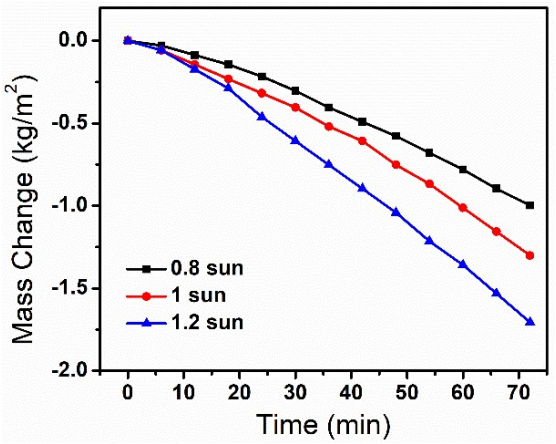

Fig. S20 Water evaporation rate curve of the MoS_2@PEI/MCE under 1 kW/m^2 irradiation.

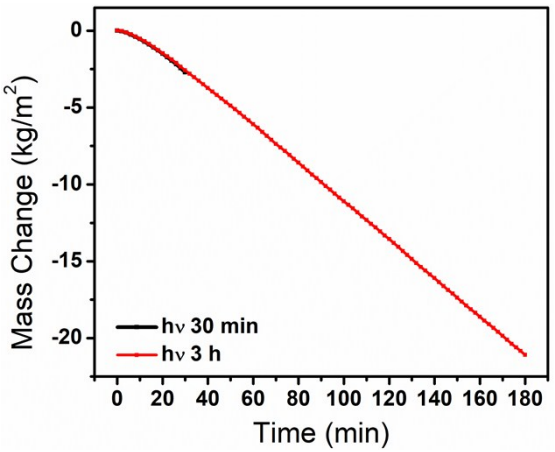

Fig. S21 Water evaporation rate curves within 30 min and 3 h of the MoS_2@PEI/MCE via 3.7 kW/m^2 irradiation.

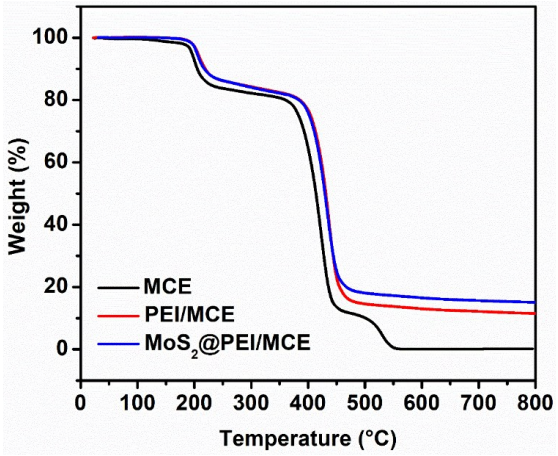

Fig. S22 TGA curves of MCE, PEI/MCE and MoS_2@PEI/MCE membranes.

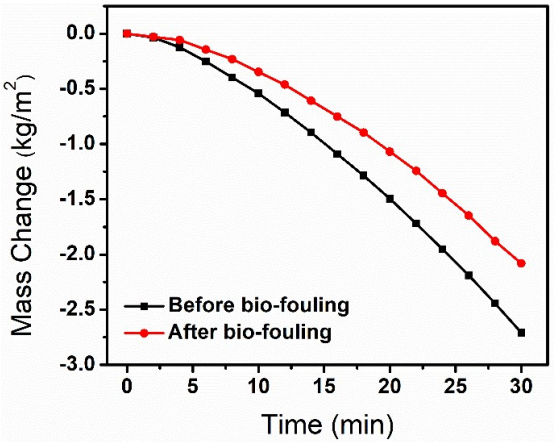

Fig. S23 Water evaporation performances under the 3.7 kW/m^2 solar irradiation of MoS_2@PEI/MCE membranes before and after bio-fouling.

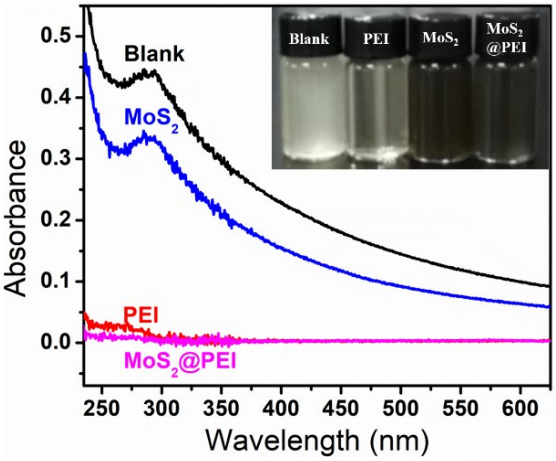

Fig. S24 UV-Vis absorption spectra and optical images (insets) of bacterial suspensions treated by blank, PEI, MoS_2 and MoS_2@PEI, respectively.

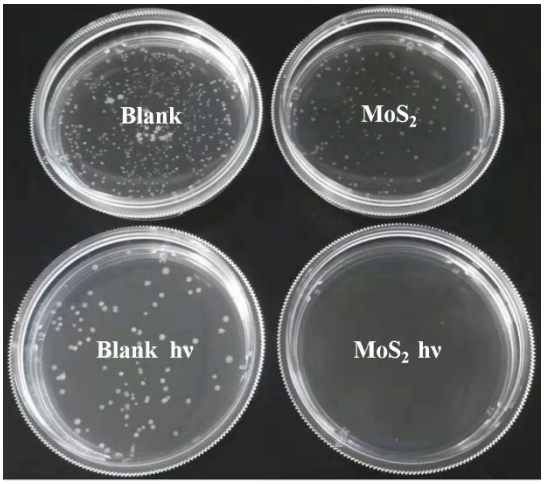

Fig. S25 Optical images of agar plates after incubating without and with the MoS_2-treated bacterial suspensions before and after irradiation for 18 min via 1 sun.

Table S1. Zeta potentials of different materials.

Samples	MoS_2	MoS_2@PEI
Zeta potential/mV	-42.4	9.3

Table S2. Comparations of the MoS_2@PEI/MCE membrane-mediated evaporation performances with some previous works of solar steam generation systems.

	Power density (kW m^{-2})	**Evaporation efficiency (%)**	**Classification of photothermal materials**	**Reference**
PDA/BNC	1	78	polymer	5
Black titania nanocages film	1	70.9	Semiconductor material	6
Plasmonic-active filter paper (PP)	10	89	Metal-based material	7
VACNT array	5	60	Carbon-based material	8
SWNT-MoS_2	5	91.5	Semiconductor material	9
F-Wood/CNTs	10	81	Carbon-based material	10
Black TiO_x-coated stainless-steel mesh	1	50.3	Semiconductor material	11
Flexible thin-film black gold membranes	20	57	Metal-based material	12
PMoS_2- CC	1	80.5	Semiconductor material	13
ce-MoS_2/BNC bilayer aerogel	5.35	81.4	Semiconductor material	14
MoS_2-based solar evaporator (MSE)	1	80	Semiconductor material	15

MoS_2@PEI/MCE	**1, 3.7**	**83, 92**	**Semiconductor material**	**This work**

References

1 Q. Jiang, L. Tian, K. K. Liu, S. Tadepalli, R. Raliya, P. Biswas, R. R. Naik and S. Singamaneni, *Adv. Mater.*, 2016, **28**, 9400-9407.
2 P. Zhang, J. Li, L. Lv, Y. Zhao and L. Qu, *ACS Nano*, 2017, **11**, 5087-5093.
3 N. Xu, X. Hu, W. Xu, X. Li, L. Zhou, S. Zhu and J, Zhu, *Adv. Mater.*, 2017, **29**, 1606762.
4 P. Zhang, J. Li, L. Lv, Y. Zhao and L. Qu, *ACS Nano*, 2017, **11**, 5087-5093.
5 Q. Jiang, H. G. Derami, D. Ghim, S. Cao, Y. Jun and S. Singamaneni, *J. Mater. Chem. A*, 2017, **5**, 18397-18402.
6 G. Zhu, J. Xu, W. Zhao and F. Huang, *ACS Appl. Mater. Inter.*, 2016, **8**, 31716-31721.
7 Z. Liu, Z. Yang, X. Huang, C. Xuan, J. Xie, H, Fu, Q, Wu, J. Zhang, X. Zhou and Y. Liu, *J. Mater. Chem. A*, 2017, **5**, 20044-20052.
8 Z. Yin, H. Wang, M. Jian, Y. Li, K. Xia, M. Zhang, C. Wang, Q. Wang, M. Ma, Q. Zheng and Y. Zhang, *ACS Appl. Mater. Inter.*, 2017, **9**, 28596-28603.
9 X. Yang, Y. Yang, L. Fu, M. Zou, Z. Li, A. Cao and Q. Yuan, *Adv. Funct. Mater.*, 2018, **28**, 1704505.
10 C. Chen, Y. Li, J. Song, Z. Yang, Y. Kuang, E. Hitz, C. Jia, A. Gong, F. Jiang, J. Y. Zhu, B. Yang, J. Xie and L. Hu, *Adv. Mater.*, 2017, **29**, 1701756.
11 M. Ye, J. Jia, Z. Wu, C. Qian, R. Chen, P. G. O'Brien, W. Sun, Y. Dong and G. A. Ozin, *Adv. Energy Mater.*, 2017, **7**, 1601811.
12 K. Bae, G. Kang, S. K. Cho, W. Park, K. Kim and W. J. Padilla, *Nat. Commun.*, 2015, **6**, 10103.
13 Z. Guo, G. Wang, X. Ming, T. Mei, J. Wang, J. Li, J. Qian and X. Wang, *ACS Appl. Mater. Inter.*, 2018, **10**, 24583-24589.
14 D. Ghim, Q. Jiang, S. Cao, S. Singamaneni and Y. Jun, *Nano Energy*, 2018, **53**, 949-957.
15 R. Chen, X. Wang, Q. Gan, T. Zhang, K. Zhu and M. Ye, *J. Mater. Chem.* A, 2019, **7**, 11177-11185.